

# KCNK5 Regulating Potassium Efflux and Inducing Pyroptosis in Corneal Epithelial Cells Through TNFSF10-Mediated Autophagy in Dry Eye

Kai Liao, Hao Zeng, Xue Yang, Dalian He, Bowen Wang, and Jin Yuan

State Key Laboratory of Ophthalmology, Zhongshan Ophthalmic Center, Sun Yat-Sen University, Guangdong Provincial Key Laboratory of Ophthalmology and Visual Science, Guangzhou, China

Correspondence: Bowen Wang, State Key Laboratory of Ophthalmology, Zhongshan Ophthalmic Center, Sun Yat-Sen University, Guangzhou, China;

[sysuwangbowen@126.com](mailto:sysuwangbowen@126.com).

Jin Yuan, State Key Laboratory of Ophthalmology, Zhongshan Ophthalmic Center, Sun Yat-Sen University, Guangzhou, China; [yuanjincornea@126.com](mailto:yuanjincornea@126.com).

KL and HZ contributed equally to this work.

**Received:** November 9, 2023

**Accepted:** January 3, 2024

**Published:** January 18, 2024

Citation: Liao K, Zeng H, Yang X, He D, Wang B, Yuan J. KCN5 regulating potassium efflux and inducing pyroptosis in corneal epithelial cells through TNFSF10-mediated autophagy in dry eye. *Invest Ophthalmol Vis Sci*. 2024;65(1):34.

<https://doi.org/10.1167/iovs.65.1.34>

**PURPOSE.** The purpose of this study was to elucidate the involvement of potassium two pore domain channel subfamily K member 5 (KCNK5)-mediated potassium efflux in the pathogenesis of dry eye and to unravel the underlying molecular mechanisms.

**METHODS.** To induce experimental dry eye in adult wild-type C57BL/6 mice, scopolamine was administered via subcutaneous injection, and the mice were subjected to desiccating stress. To create an in vitro model of dry eye, desiccation stress was applied to the human corneal epithelial cell line (HCE-T). Intracellular potassium concentration was quantified using inductively coupled plasma mass spectrometry. Cellular death was assessed through lactate dehydrogenase assays. Gene expression profiling was conducted through both RNA sequencing and quantitative real-time PCR. Protein analysis was carried out through Western blotting and immunofluorescence staining. Assessment of the corneal epithelial defect area was conducted through fluorescein sodium staining. Tear secretion was quantified using the phenol red cotton thread method.

**RESULTS.** Potassium efflux was observed to further facilitate corneal epithelial pyroptosis. KCN5 exhibited upregulation in both in vivo and in vitro models of dry eye. The overexpression of KCN5 was observed to induce potassium efflux and activate the NLR family pyrin domain containing 3 (NLRP3) inflammasome-mediated pyroptosis in vitro. Silencing KCN5 effectively mitigated pyroptosis in dry eye. Additionally, the overexpression of KCN5 results in the downregulation of TNF superfamily member 10 (TNFSF10) and subsequent impairment of autophagy. TNFSF10 supplementation could promote autophagy and mitigate pyroptosis in dry eye.

**CONCLUSIONS.** The upregulation of KCN5 mediates TNFSF10 to impair autophagy and induce pyroptosis in dry eye. Consequently, targeting KCN5 may represent a novel and promising approach to therapeutic intervention in the management of dry eye.

**Keywords:** KCN5, potassium efflux, pyroptosis, autophagy, dry eye

Dry eye is a multifactorial chronic ocular condition, and it presents with a range of clinical symptoms, including ocular pain, itching, foreign body sensation, and blurred vision. These symptoms significantly impact the daily lives of a substantial portion of the global population, estimated to be between 5% and 35%.<sup>1</sup> Chronic inflammation is a pivotal factor in the onset and progression of dry eye.<sup>2</sup> Desiccation stress, leading to heightened ocular dryness, has been observed to incite inflammation on the ocular surface, thereby amplifying the overall inflammatory response.<sup>3</sup> Nevertheless, a comprehensive understanding of the specific pathogenetic mechanisms responsible for inflammation induced by desiccation stress in the context of dry eye remains an area in need of further investigation.

Pyroptosis is a form of programmed cell death that relies on the gasdermin protein-mediated pore-forming activity on the cell membrane, which is induced by inflammasomes.<sup>4</sup> Recent research has been yielding growing evidence of a strong association between pyroptosis and dry eye.<sup>5-7</sup> In our

prior research, we established that IFN- $\gamma$  could enhance the pyroptosis of corneal epithelial cells in dry eye.<sup>8</sup> Nonetheless, numerous inquiries pertaining to the activation of pyroptosis in the context of dry eye persist and require further elucidation.

Potassium efflux represents a critical step that is imperative for the activation of the NLRP3 inflammasome mediated pyroptosis in response to various extracellular stimuli.<sup>9</sup> Typically, the outflow of potassium ions is facilitated by the activation of potassium channels. Potassium channel activity is associated with the progression of some eye diseases. Potassium two pore domain channel subfamily K (KCNK) family genes encode unique channel subunits with two pore-forming P domains. These two-pore domain potassium channels comprise a major and structurally distinct subset of mammalian potassium channel superfamily, which contribute to the background leak currents, responsible for maintaining the resting membrane potential in nearly all cells. They are regulated by various physical, chemical, and

biological stimuli and implicated in multiple physiological processes.<sup>10</sup> KCNK9 regulates the intrinsic excitability and the light sensitivity of retinal ganglion cells (RGCs) by sensing neuronal activity-dependent extracellular acidification.<sup>11</sup> KCNQ5 mutation could lead to rat retinal degeneration.<sup>12</sup> KCa3.4 activation could lead to mice corneal fibrosis.<sup>13</sup> Nonetheless, the connection between potassium ion efflux and pyroptosis in corneal epithelial cells, as well as the identification of the specific potassium ion channel that plays a central role in this process, remains uncharted territory in the existing literature.

Autophagy is a self-degradation mechanism intrinsic to mammalian cells, instrumental in mitigating excessive inflammation through the attenuation of inflammatory factor secretion within the tear film.<sup>14</sup> Research has elucidated the pivotal role of autophagy regulation as a mechanistic component in the pathogenesis of dry eye disease, synergistically intertwined with the inflammatory cascade.<sup>15</sup> In our prior research, we established that excessive reactive oxygen species release through DNA damage-inducible transcript 4 (DDIT4) induction can lead to impaired autophagy and decreased cell viability in dry eye disease.<sup>16</sup> Recent investigations indicate a close inter-relationship between the activity of potassium channels and the modulation of autophagic processes.<sup>17</sup> However, the precise causative link between potassium channel activation and aberrant autophagic processes in corneal epithelial cells, and its consequent contribution to the onset of dry eye, remains unclear.

In this study, we explored the role of potassium channel KCNK5 in the development of dry eye. Afterward, we explored the molecular mechanism between KCNK5 and pyroptosis. Overall, we founded that KCNK5 plays an important role in the pathogenesis of dry eye.

## METHODS

### Dry Eye Mice Model and Treatment

Adult C57BL/6 (wildtype) mice were procured from Guangzhou Vital River Laboratory Animal Company. The execution of experimental protocols adhered to the guidelines provided by the Association for Research in Vision and Ophthalmology (ARVO) for the Utilization of Animals in Ophthalmic and Vision Research. The ethical approval for the experimental procedures was granted by the Ethics Committee of Zhongshan Ophthalmic Center. The dry eye mice model was established following the method previously described.<sup>18</sup> Mice received 3 daily subcutaneous injections of 0.5 mg/0.2 mL scopolamine hydrobromide (Sigma-Aldrich, Allentown, PA, USA) for 7 consecutive days. During this period, the mice were accommodated in cages featuring a perforated plastic screen on one side, facilitating airflow from a fan positioned at a distance of 6 inches for 16 hours per day, sustained over 1 day. Room humidity levels were maintained within the range of 20% to 30%. The criterion for the successful establishment of a dry eye mice model is the presence of evident epithelial defects in the central cornea, as revealed by corneal sodium fluorescein staining, along with a significant reduction in tear secretion.

After dry eye mice models were established, dry eye mice were randomly assigned to different groups (15 mice per group). In the first part of the experiment, the mouse groups were categorized as follows: control (Ctrl) group, dry eye (DE) group, combined dry eye with negative control

siRNA treatment (DE+siNC) group, and combined dry eye with KCNK5 siRNA treatment (DE+siKCNK5) group. In the second part of the experiment, the mouse groups were categorized as follows: control (Ctrl) group, dry eye (DE) group, combined dry eye with PBS treatment (DE+PBS) group, and combined dry eye with rhTNFSF10 treatment (DE+TNFSF10) group. Mice were injected subconjunctivally (5  $\mu$ L per eye) with KCNK5 siRNA (10  $\mu$ M) or recombinant human TNFSF10 (rhTNFSF10; 10  $\mu$ g/mL; R&D Systems, Minneapolis, MN, USA) once a day for 7 consecutive days. Scrambled siRNA or PBS was subconjunctivally as control. In vivo transfection of siRNA was performed using the InvivoFectamine 3.0 reagent (Thermo Fisher Scientific, Waltham, MA, USA). The dose-dependent response was evaluated through the subconjunctival administration of KCNK5 siRNA at concentrations of 1, 5, and 10  $\mu$ M, or rhTNFSF10 at concentrations of 1, 5, and 10  $\mu$ g/mL. Immunofluorescence staining results demonstrated that KCNK5 siRNA at 10  $\mu$ M or rhTNFSF10 at 10  $\mu$ g/mL exhibited the most pronounced inhibition of KCNK5 or recovery of TNFSF10. These specific doses were subsequently used in subsequent experiments (Supplementary Fig. S1). Slit-lamp biomicroscopy examination was performed on days 0, 3, and 7 after topically therapy. On day 7, the mice were harvested for subsequent experiments including Western blot and immunofluorescence staining. Quantification analysis of the corneal epithelial defect area was performed using ImageJ software.

### Tear Secretion Test

Tear secretion was evaluated using the phenol red thread method (Jingming, China) on the seventh day post dry eye mouse model induction. In this technique, the phenol red thread was delicately positioned at the palpebral conjunctiva of the lower eyelid, proximate to the lateral canthus, and maintained for a period of 15 seconds.

### Cell Culture and Treatment

Human immortalized corneal epithelial cell line (HCE-T) was kindly provided by Prof. Wu of Sun Yat-Sen University. The basic cell culture medium contained DMEM/F12 (Gibco, Waltham, MA, USA), 10% fetal bovine serum (Gibco, USA), and 1% streptomycin /penicillin (Gibco, USA).

Potassium efflux cell model was established following the method previously.<sup>19</sup> In brief, nigericin (10  $\mu$ M; MedChem-Express [MCE], Hong Kong, China) was added into the cell culture medium. The cell groups were categorized as follows: control group, nigericin group, combined nigericin with quinine (10  $\mu$ M) group, and combined nigericin with quinine (100  $\mu$ M) group. After treatment for 24 hours, the cells were harvested for subsequent experiments.

Desiccation stress in vitro model was established following the method previously described.<sup>20</sup> In brief, the medium was completely aspirated from HCE-T cells and air dried for 10 minutes. Further, the cell culture medium was replenished and cells were treated with or without KCNK5 siRNA for 24 hours. Subsequently, the cells were harvested for subsequent experiments.

### KCNK5 Overexpression

The KCNK5 overexpression lentivirus vector and empty vector were designed and constructed by Tsingke Biotechnology (Beijing, China). The lentiviral vectors were

introduced into HCE-T cells following the manufacturer's guidelines. Briefly, HCE-T cells were initially seeded in 6-well plates and allowed to reach a confluence of 40% to 60%. Subsequently, the cells were subjected to lentiviral transfection. Following a 48-hour incubation post-transfection, the cells were subcultured for subsequent experiments.

### RNA Interference

Human KCNK5 siRNA were designed by Tsingke Biotechnology (Guangzhou, China). A scrambled siRNA was used as a nonspecific siRNA control. Lipofectamine RNAiMAX (Invitrogen, Carlsbad, CA, USA) and siRNA were incubated with Opti-MEM (Invitrogen, USA). The mixture was added to cell culture medium and continued to culture for 24 hours. The siRNA primers used in this study are cataloged in Supplementary Table S1.

### Lactate Dehydrogenase Assay

Cell death was evaluated using LDH kit (Beyotime, Haimen, Jiangsu, China). HCE-T cells were inoculated in 96-well plates with the density at  $1 \times 10^4$  cells/mL. HCE-T cells were treated differently according to groups and then collected the cell supernatant. The cell supernatant was mixed with LDH solution and incubated at 37°C for 30 minutes. The OD at 490 nm was detected with a microplate reader.

### Intracellular Elemental Analysis

Intracellular elemental analysis was performed following the method described previously.<sup>21</sup> HCE-T cells were seeded in 24-well plates. After desiccation stress treatment, culture media were thoroughly aspirated and cells were extracted 30 minutes in 3% ultrapure HNO<sub>3</sub>. Intracellular potassium measurements were performed by inductively coupled plasma spectrometry (Guangzhou Hexin Instrument Co., Ltd., Guangzhou, China) using yttrium as internal standard. To ensure precise measurement of intracellular ion levels, a control procedure was executed within each experiment to ascertain the residual extracellular ion content after aspiration. This value was subsequently deducted from all measurements to obtain accurate results.

### RNA-Sequencing Analysis

Total RNA was extracted from mice corneal tissue and HCE-T cells using Trizol (Thermo Fisher Scientific, USA). RNA-sequencing was performed by GENE DENOVO tech Co., Ltd. (Guangzhou, China). The differentially expressed genes (DEGs) were identified using the DESeq2 analysis with the filter criteria  $|\log_2 \text{fold change}| > 1$  and  $P \text{ value} < 0.05$ . Gene set enrichment analysis (GSEA) analysis was performed using GSEA software (<http://software.broadinstitute.org/gsea/>).

### Quantitative Real-Time PCR

Total RNA was extracted from HCE-T cells samples using Trizol (Thermo Fisher Scientific, USA). Reverse transcription was carried out following SuperScript reverse transcription kit (Vazyme, China). QRT-PCR was performed using SYBR Green reagents (Vazyme, China). The primers used in this study are cataloged in Supplementary Table S1.

### Western Blot

Total proteins were extracted in RIPA buffer containing 1% proteinase inhibitor (Thermo Fisher Scientific, USA). Proteins were separated by 12% SDS-PAGE gels and electronically transferred to 0.22  $\mu\text{m}$  PVDF membranes (Millipore, Chicago, IL, USA). Membranes were blocked with block solution (Beyotime, China) for 1 hour at room temperature. After that, the membranes were incubated with the primary antibodies overnight. The next day, the membranes were washed 3 times with TBST, and the secondary antibody was incubated for 1 hour at room temperature. The blot intensities were analyzed by ImageJ software (National Institutes of Health, Bethesda, MD, USA). The antibodies used in this study are cataloged in Supplementary Table S2.

### Immunofluorescence Staining

Mice corneal tissue paraffin sections and HCE-T cell samples were deparaffinized, rehydrated, and immersed. Afterward, the sections were treated with 3% BSA for 2 hours at room temperature for blocking and permeabilized with 0.5% Triton X-100 for another 5 minutes. The sections were incubated with primary antibody at 4°C overnight. The next day, the sections were washed with PBST 3 times, and then incubated with secondary antibody for 1 hour at room temperature. Nuclear staining was performed with DAPI for another 5 minutes. The antibodies used in this study are cataloged in Supplementary Table S2.

### Transmission Electron Microscopy

HCE-T cell samples were fixed with glutaraldehyde and sodium cacodylate at 4°C overnight. The next day, the cells were treated with 1% OsO<sub>4</sub>. Afterward, cells were dehydrated in ethanol and embedded in epoxy resin. The samples were examined by Hitachi transmission electron microscope system (HT7700; Hitachi, Hitachi City, Japan).

### Statistical Analysis

Statistical analyses were performed using Student's *t*-test and ANOVA tests. The results of analysis were performed using GraphPad Prism 8.3 software (GraphPad Software Inc., San Diego, CA, USA). Any  $P < 0.05$  was considered as statistically significant.

## RESULTS

### Potassium Efflux Induces Pyroptosis in Corneal Epithelial Cells

To investigate alterations in intracellular potassium levels in the in vitro dry eye model, inductively coupled plasma mass spectrometry was used. The outcomes revealed a notable and statistically significant reduction in intracellular potassium levels subsequent to desiccation stress treatment (Fig. 1A). Additionally, intracellular concentrations of sodium, magnesium, zinc, and phosphorus ions exhibited a decrease, whereas copper and calcium ions did not display significant alterations.

Nigericin could induce potassium efflux, subsequently activating the NLRP3 inflammasomes.<sup>22,23</sup> Quinine, serving as a potassium channel inhibitor, has the capability to impede potassium efflux, thus modulating the activation

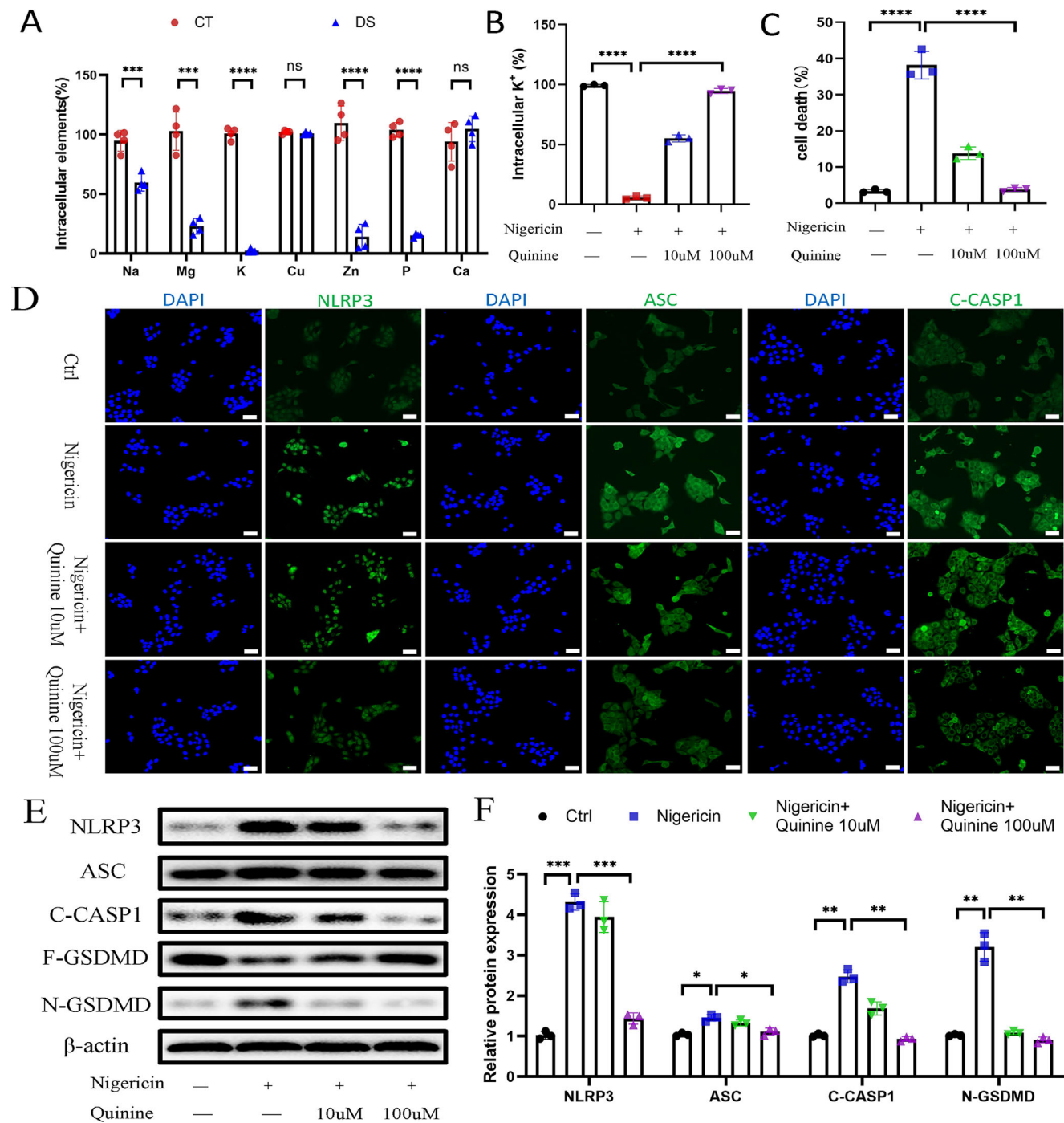


**FIGURE 1.** Potassium efflux induces pyroptosis in corneal epithelial cells. (A) Intracellular elemental analysis of HCE-T cells following desiccation stress treatment ( $n = 4/\text{group}$ ). (B) Intracellular potassium concentration dynamics in HCE-T cells following nigericin and quinine treatment ( $n = 3/\text{group}$ ). (C) LDH assay results in HCE-T cells following nigericin and quinine treatment ( $n = 3/\text{group}$ ). (D) Representative immunofluorescence staining of NLRP3, ASC, and C-CASP1 in HCE-T cells. (E) and (F) Western blot and quantitative analysis results of NLRPS, ASC, C-CASP1, F-GSDMD, and N-GSDMD in HCE-T cells ( $n = 3/\text{group}$ ). Scale bar = 100  $\mu\text{m}$ . Error bars = standard deviation. ns, no significant difference. \* $P < 0.05$ , \*\* $P < 0.01$ , \*\*\* $P < 0.001$ , \*\*\*\* $P < 0.0001$ .

of this pivotal pathway.<sup>19,24</sup> In our study, we observed a reduction in intracellular potassium concentration subsequent to nigericin treatment at a concentration of 10  $\mu\text{M}$ . This potassium efflux was effectively mitigated when quinine, administered at a concentration of 100  $\mu\text{M}$ , was applied to corneal epithelial cells (Fig. 1B). The percentage of cell deaths was elevated following potassium efflux.

Significantly, quinine treatment was able to attenuate the increase in cell death (Fig. 1C). Immunofluorescence staining results demonstrated an upregulation of NLRP3, apoptosis-associated speck-like protein (ASC), and cleaved-caspase 1 (C-CASP1) following the induction of potassium efflux by nigericin. Treatment with quinine effectively downregulated the expression of these proteins (Fig. 1D). Additionally, West-

ern blot data demonstrated increased levels of NLRP3, ASC, C-CASP1, and N-terminus gasdermin D (N-GSDMD) following potassium efflux, which were notably ameliorated by the administration of quinine (see Figs. 1E, 1F). These findings strongly suggest that the inhibition of potassium efflux has the potential to effectively attenuate pyroptosis in corneal epithelial cells.

### KCNK5 Exhibited Upregulation in Both In Vivo and In Vitro Models of Dry Eye

To explore the expression of KCNK family genes in dry eye, we performed RNA-seq assays on an in vivo model of dry eye. GSEA analysis revealed upregulation of potassium channel activity in dry eye mice (Fig. 2A). The heatmap results showed the expression of KCNK family genes in normal mice and dry eye mice (Fig. 2B). The quantitative PCR (qPCR) results revealed that KCNK5 exhibited the most pronounced upregulation in dry eye mice group when compared to the control group (Fig. 2C). Additionally, KCNK1 expression was also upregulated, whereas other potassium channels, such as KCNK4, KCNK6, and KCNK7, did not exhibit significant changes. Immunofluorescence staining results demonstrated an upregulation of KCNK5 in dry eye mice (Fig. 2G). Besides, we also explored the expression of KCNK family genes in HCE-T cells. GSEA analysis revealed upregulation of potassium channel activity in desiccation stress group (Fig. 2D). The heatmap results showed the expression of KCNK family genes in the control group and the desiccation stress group (Fig. 2E). The qPCR results revealed that KCNK5 exhibited the most pronounced upregulation in the desiccation stress group. KCNK1 showed an increase in expression, whereas other potassium channels, such as KCNK2, KCNK6, and KCNK4, did not exhibit significant changes (Fig. 2F). Immunofluorescence staining results demonstrated an upregulation of KCNK5 in HCE-T cells following desiccation stress treatment (Fig. 2H). It is evident that KCNK5 showed upregulation in both in vivo and in vitro dry eye models.

### KCNK5 Overexpression Induces Pyroptosis in Corneal Epithelial Cells

To investigate the impact of KCNK5 in corneal epithelial cells, we used lentivirus transfection to overexpress KCNK5 in HCE-T cells. The outcomes revealed a reduction in intracellular potassium concentration following KCNK5 overexpression, a response effectively mitigated by quinine (Fig. 3A). The incidence of cell death increased after KCNK5 overexpression but was mitigated upon the administration of quinine (Fig. 3B). Furthermore, qPCR results demonstrated that KCNK5 overexpression led to the upregulation of inflammatory factors IL-6, IL-1A, and IL-1B, with this response also being successfully inhibited by quinine (Fig. 3C). Immunofluorescence staining results revealed a significant upregulation of NLRP3, ASC, and C-CASP1 in response to KCNK5 overexpression, and this upregulation was subsequently attenuated by quinine treatment (Fig. 3D). In alignment with this, Western blot data indicated elevated levels of NLRP3, ASC, C-CASP1, and N-GSDMD following KCNK5 overexpression. Notably, the administration of quinine effectively mitigated this upregulation (Figs. 3E, 3F). These compelling findings collectively indicate that KCNK5 overexpression induces potassium efflux, subsequently triggering pyroptosis in corneal epithelial cells.

### Silencing KCNK5 Inhibits Pyroptosis in Dry Eye

The forementioned results conclusively establish that the overexpression of KCNK5 is causally linked to pyroptosis in corneal epithelial cells. Consequently, we posited that the silencing of KCNK5 might serve as an effective strategy to inhibit pyroptosis. In the in vitro model of dry eye, our results indicated a substantial decrease in intracellular potassium concentration upon exposure to desiccation stress, followed by its amelioration through the silencing of KCNK5 (Fig. 4A). The frequency of cell death exhibited an elevation subsequent to the treatment with desiccation stress, which was subsequently alleviated upon the inhibition of KCNK5 (Fig. 4B). Moreover, qPCR results unveiled a significant increase in the expression of pro-inflammatory cytokines, including IL-6, IL-1A, and IL-1B, as a consequence of desiccation stress treatment, and this upregulation was subsequently ameliorated by the inhibition of KCNK5 (Fig. 4C). The results from immunofluorescence staining displayed a pronounced elevation in the expression of NLRP3, ASC, and C-CASP1 within HCE-T cells upon desiccation stress treatment, and this upregulation was subsequently alleviated by the inhibition of KCNK5 (Fig. 4D). Consistent with these observations, Western blot analysis revealed elevated levels of NLRP3, ASC, C-CASP1, and N-GSDMD after desiccation stress treatment, which were subsequently ameliorated upon the inhibition of KCNK5 (Figs. 4E, 4F).

In addition, we conducted tests to evaluate the impact of silencing KCNK5 in dry eye mice. Following the silencing of KCNK5 in dry eye mice, there was a notable reduction in the corneal epithelial defect area (Figs. 5A, 5B). Furthermore, the inhibition of KCNK5 in the dry eye mice model resulted in a partial restoration of tear secretion (Fig. 5C). Immunofluorescence staining results further supported these observations by revealing a downregulation of NLRP3, ASC, and C-CASP1 in dry eye mice following KCNK5 silencing (Fig. 5D). In concordance with these findings, Western blot data indicated downregulated levels of NLRP3, ASC, C-CASP1, and N-GSDMD subsequent to silencing KCNK5 in dry eye mice (Figs. 5E, 5F). These findings indicate that silencing KCNK5 effectively inhibits pyroptosis and alleviates symptoms in dry eye mice.

### KCNK5 Mediates TNFSF10 to Impair Autophagy and Induce Pyroptosis in Corneal Epithelial Cells

To explore the molecular mechanism of pyroptosis induced by KCNK5, we performed transcriptome sequencing on the control vector group, KCNK5 overexpression group. GSEA analysis revealed downregulation of autophagy pathway in KCNK5 overexpression group (Fig. 6A). We screened out the top 10 significantly downregulated differentially expressed genes in autophagy pathway. Heatmap result showed that only TNFSF10 was downregulated upon KCNK5 overexpression and reversed after silencing KCNK5 (Fig. 6B). Hence, we hypothesize that KCNK5 promotes pyroptosis through TNFSF10. The TNFSF10 has also been linked to the promotion of autophagy.<sup>25</sup> Therefore, it is reasonable to postulate that the overexpression of KCNK5 may hinder autophagy by inhibiting TNFSF10. The transmission electron microscopy results illustrated an abnormal accumulation of autophagosomes in the KCNK5 overexpression group, and, notably, supplementation of TNFSF10 was found to reduce this accumulation (Fig. 6C). Additionally, Western blot results indicated a decrease in the

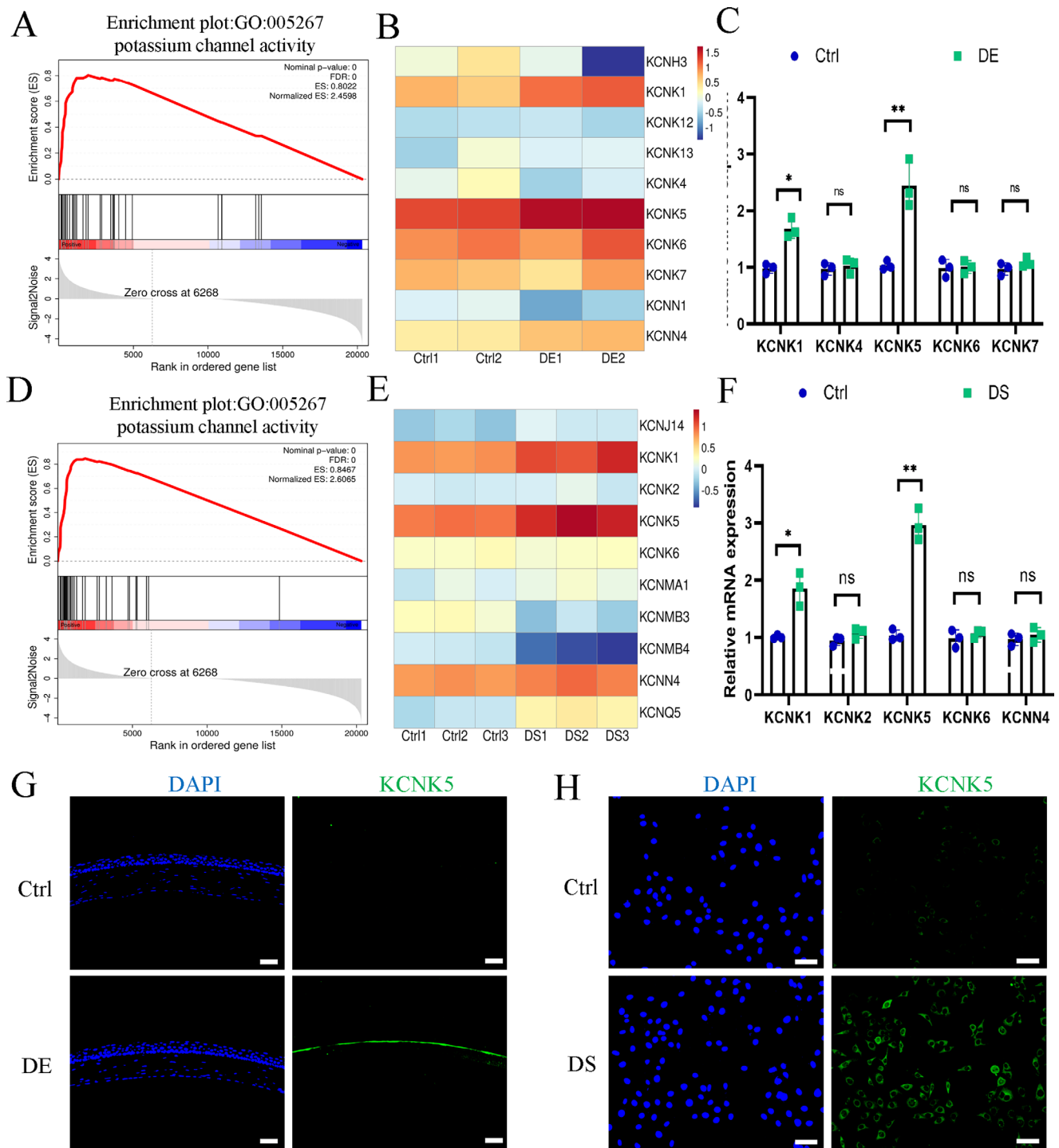


**FIGURE 2.** KCNK5 exhibited upregulation in both in vivo and in vitro models of dry eye. **(A)** GSEA analysis of potassium channel activity in the control group and the dry eye mice group. **(B)** Heatmap depicting the expression of KCNK family genes in the control group and the dry eye mice group ( $n = 3/\text{group}$ ). **(C)** Quantitative PCR results demonstrated an upregulation of KCNK5 in dry eye mice ( $n = 3/\text{group}$ ). **(D)** GSEA analysis of potassium channel activity in the control group and the desiccation stress group. **(E)** Heatmap depicting the expression of KCNK family genes in the control group and the desiccation stress group ( $n = 3/\text{group}$ ). **(F)** Quantitative PCR results demonstrated an upregulation of KCNK5 in the desiccation stress group ( $n = 3/\text{group}$ ). **(G)** Representative immunofluorescence staining of KCNK5 in normal mice and dry eye mice. **(H)** Representative immunofluorescence staining of KCNK5 in HCE-T cells. Scale bar = 100  $\mu\text{m}$ . Error bars = standard deviation. ns, no significant difference. \* $P < 0.05$ , \*\* $P < 0.01$ , \*\*\* $P < 0.001$ , \*\*\*\* $P < 0.0001$ .

levels of NLRP3, ASC, C-CASP1, N-GSDMD, SQSTM1, and LC3-II in KCNK5 overexpression group. Importantly, the supplementation of TNFSF10 was observed to counteract the effect of KCNK5 overexpression (Figs. 6D, 6E). These find-

ings suggest that the overexpression of KCNK5 can impair cell autophagy and induce pyroptosis, and the supplementation of TNFSF10 can restore autophagy and mitigate pyroptosis.

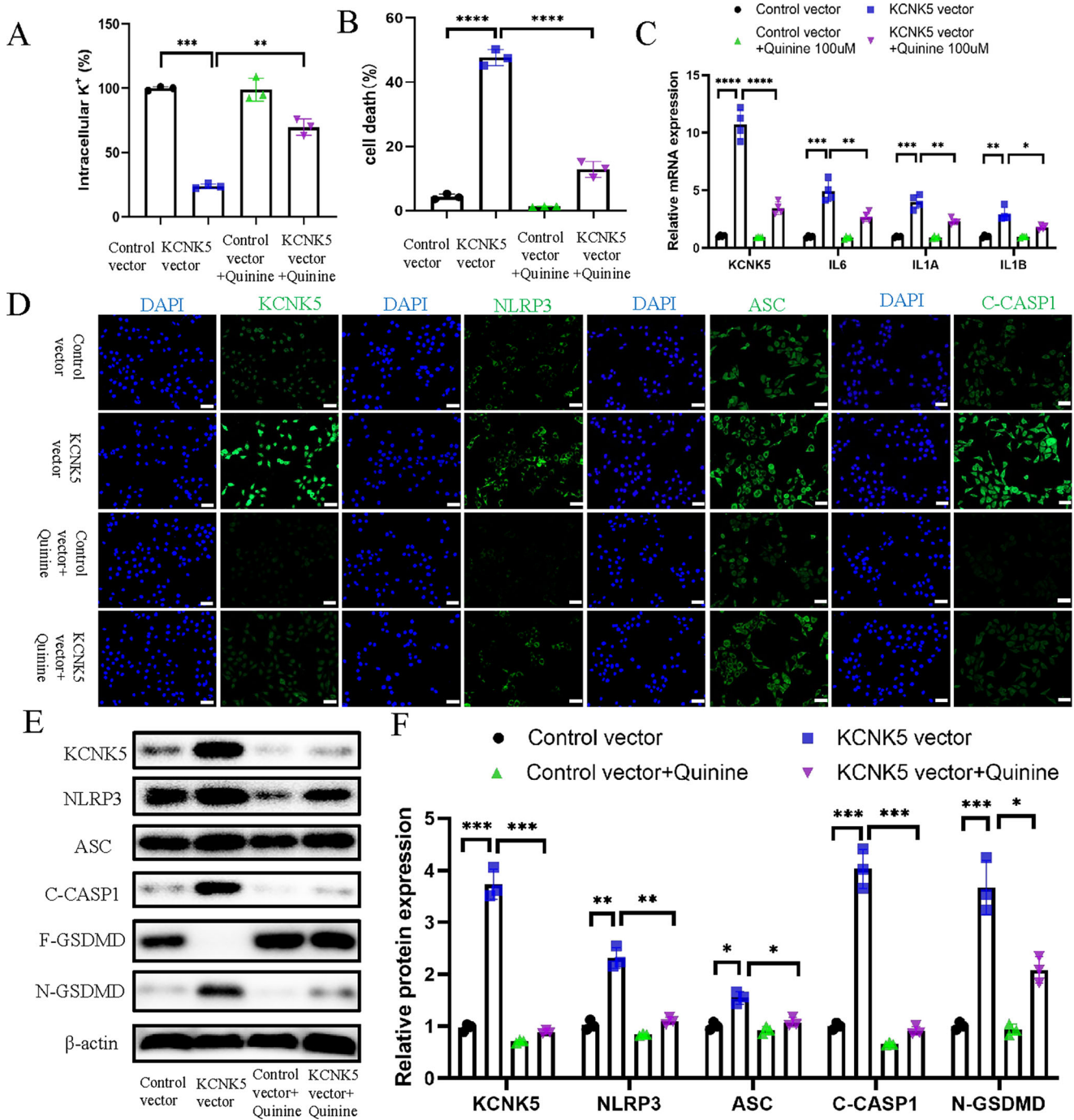


**FIGURE 3.** Overexpression of KCNK5 induces pyroptosis in corneal epithelial cells. (A) Intracellular potassium concentration dynamics in HCE-T cells upon KCNK5 overexpression and quinine treatment ( $n = 3/\text{group}$ ). (B) LDH assay results in HCE-T cells following KCNK5 overexpression and quinine treatment ( $n = 3/\text{group}$ ). (C) The mRNA level of KCNK5, IL-6, IL-1A, and IL1B in HCE-T cells ( $n = 4/\text{group}$ ). (D) Representative immunofluorescence staining of KCNK5, NLRP3, ASC, and C-CASP1 in the control and the KCNK5 overexpression groups. (E) and (F) Western blot and quantitative analysis results of KCNK5, NLRPS, ASC, C-CASP1, F-GSDMD, and N-GSDMD in HCE-T cells ( $n = 3/\text{group}$ ). Scale bar = 100  $\mu\text{m}$ . Error bars = standard deviation. ns, no significant difference. \* $P < 0.05$ , \*\* $P < 0.01$ , \*\*\* $P < 0.001$ , \*\*\*\* $P < 0.0001$ .

**TNFSF10 Promotes Autophagy and Mitigates Pyroptosis in Dry Eye Mice**

Next, we sought to investigate the impact of TNFSF10 in dry eye mice. The results of our study unveiled that the rhTNFSF10 subconjunctival injection led to a signifi-

cant reduction in the corneal epithelial defect area in dry eye mice (Figs. 7A, 7B). Additionally, there was a partial restoration of tear secretion observed following the administration of rhTNFSF10 subconjunctival injection (Fig. 7C). The immunostaining of corneal tissue unveiled a significant downregulation in the protein levels of NLRP3, ASC, and

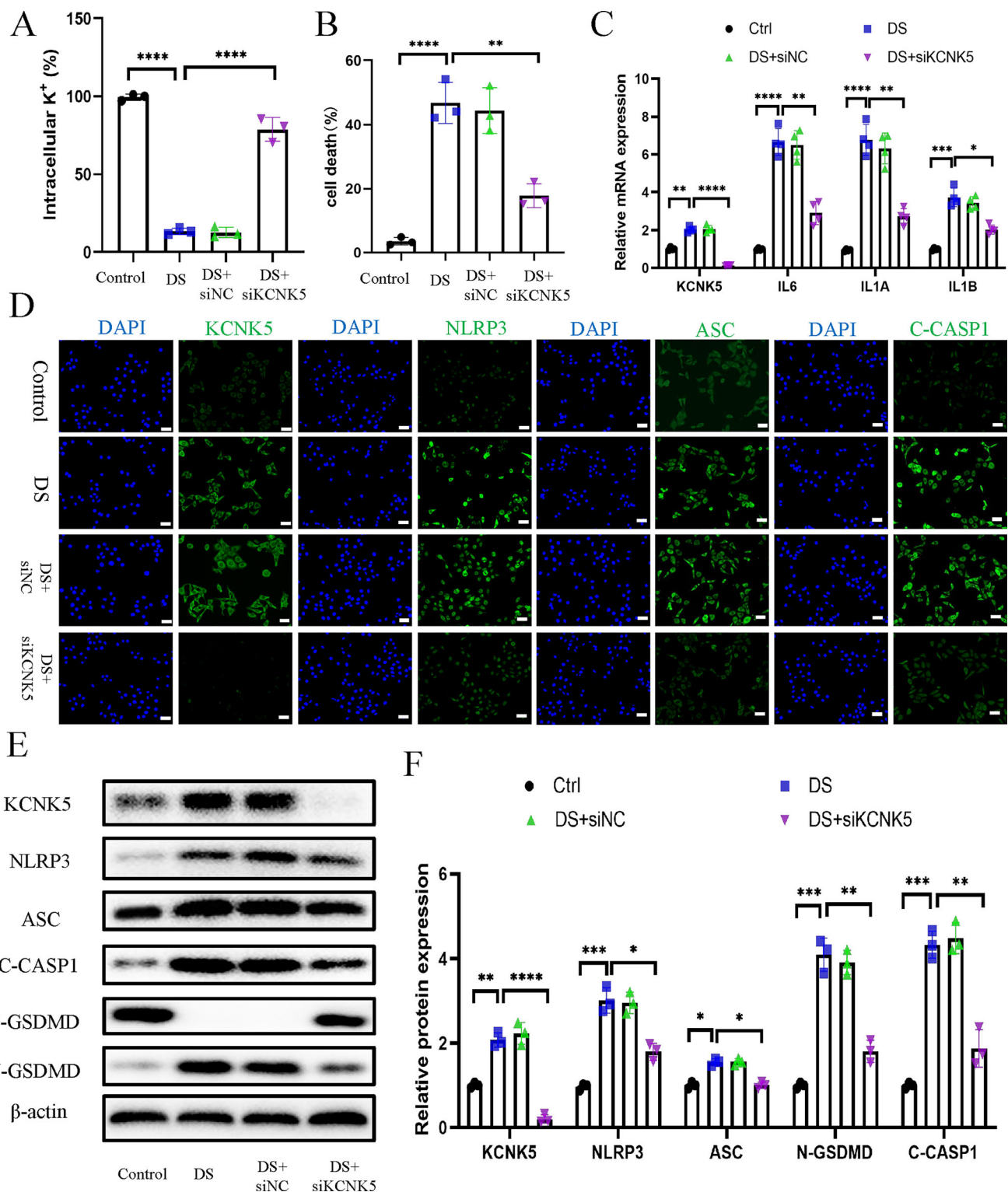


**FIGURE 4.** Silencing KCNK5 inhibits pyroptosis in corneal epithelial cells. **(A)** Intracellular potassium concentration dynamics in HCE-T cells upon desiccation stress and KCNK5 siRNA treatment ( $n = 3/\text{group}$ ). **(B)** LDH assay results in HCE-T cells upon desiccation stress and KCNK5 siRNA treatment ( $n = 3/\text{group}$ ). **(C)** The mRNA level of KCNK5, IL-6, IL-1A, and IL-1B in HCE-T cells ( $n = 4/\text{group}$ ). **(D)** Representative immunofluorescence staining of KCNK5, NLRP3, ASC, and C-CASP1 in HCE-T cells. **(E)** and **(F)** Western blot and quantitative analysis results of KCNK5, NLRP3, ASC, C-CASP1, F-GSDMD, and N-GSDMD in HCE-T cells ( $n = 3/\text{group}$ ). Scale bar = 100  $\mu\text{m}$ . Error bars = standard deviation. ns, no significant difference. \* $P < 0.05$ , \*\* $P < 0.01$ , \*\*\* $P < 0.001$ , \*\*\*\* $P < 0.0001$ .

C-CASP1, whereas TNFSF10 showed an upregulation after rhTNFSF10 subconjunctival injection (Fig. 7D). These obser-

variations were corroborated by Western blot results, which demonstrated decreased levels of NLRP3, ASC, N-GSDMD,



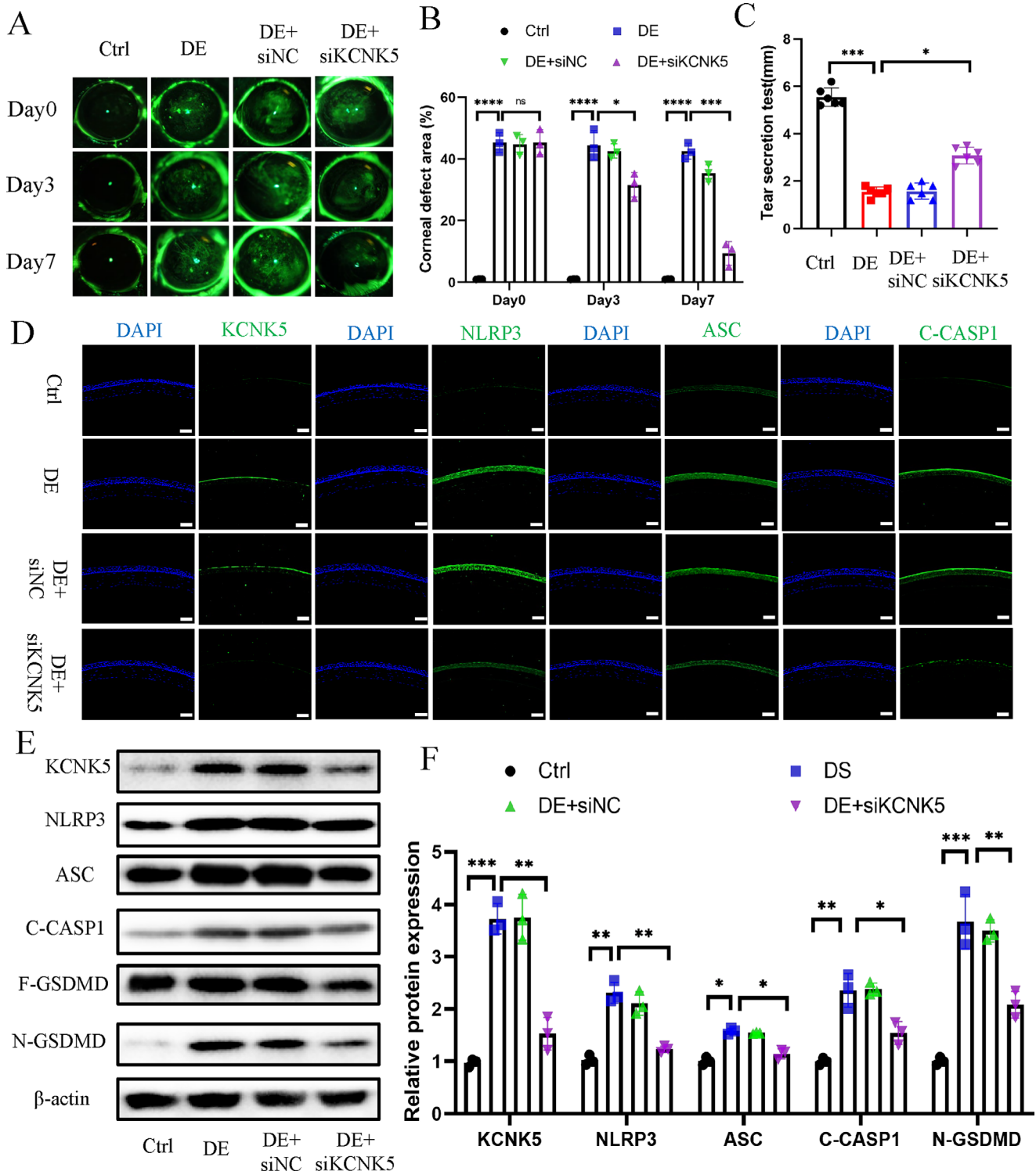


**FIGURE 5.** Silencing KCNK5 inhibits pyroptosis in dry eye mice. (A) Representative corneal fluorescein staining images in dry eye mice following treatment with scrambled siRNA and KCNK5 siRNA treatment on days 0, 3, and 7 ( $n = 3/\text{group}$ ). (B) Quantitative analysis of the corneal defect area percentage ( $n = 3/\text{group}$ ). (C) Tear secretion test in dry eye mice ( $n = 6/\text{group}$ ). (D) Representative immunofluorescence staining of KCNK5, NLRP3, ASC, and C-CASP1 in mice. (E) and (F) Western blot and quantitative analysis results of KCNK5, NLRP3, ASC, C-CASP1, F-GSDMD, and N-GSDMD in mice ( $n = 3/\text{group}$ ). Scale bar = 100  $\mu\text{m}$ . Error bars = standard deviation. ns, no significant difference.  $*P < 0.05$ ,  $**P < 0.01$ ,  $***P < 0.001$ ,  $****P < 0.0001$ .

C-CASP1, SQSTM1, and LC3-II, alongside an upregulation of TNFSF10 after rhTNFSF10 subconjunctival injection treatment (Figs. 7E, 7F). These findings collectively suggest that

rhTNFSF10 subconjunctival injections have the capacity to mitigate pyroptosis in dry eye mice by restoring impaired autophagy.

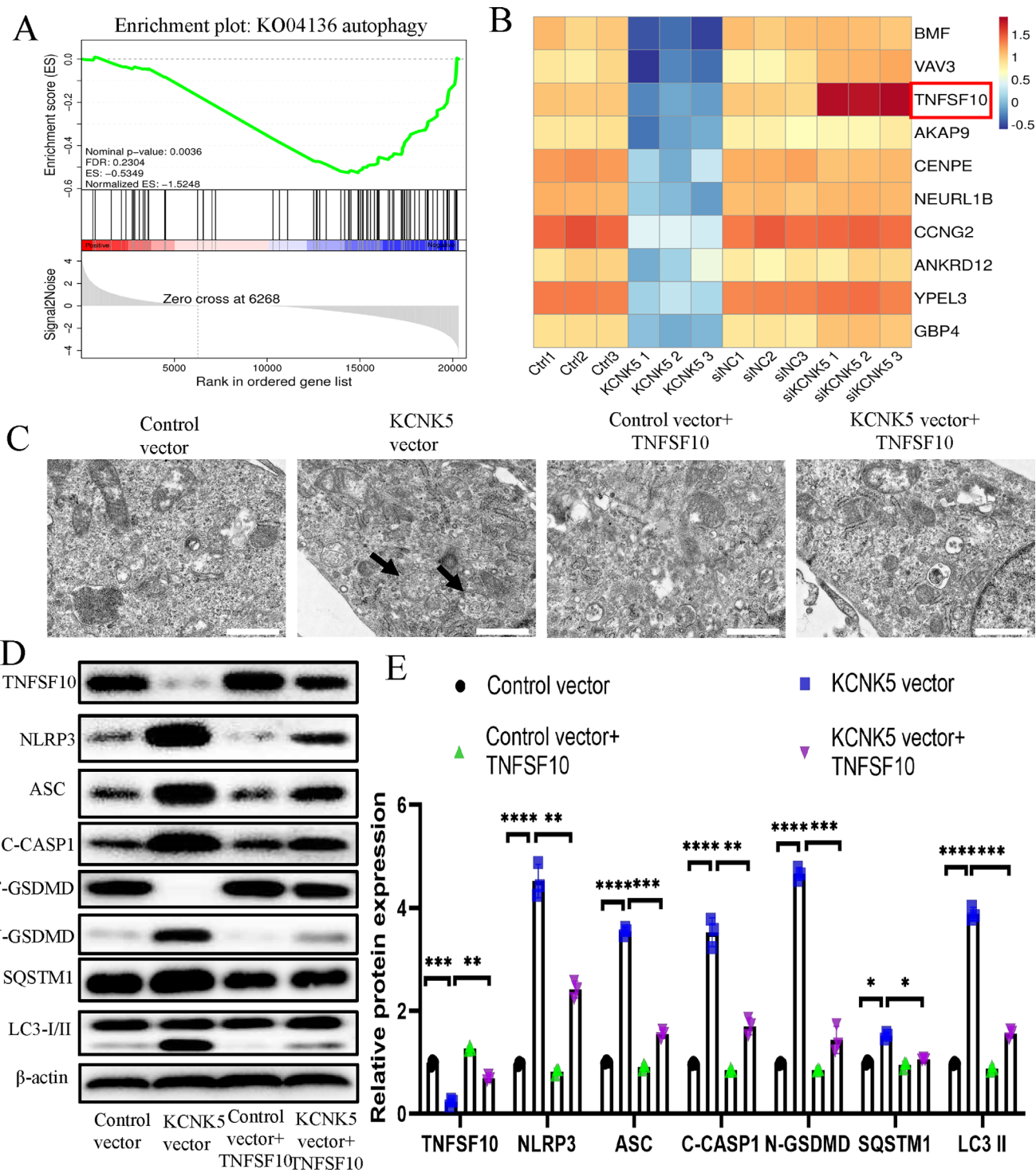


**FIGURE 6.** KCN5 mediates TNFSF10 to impair autophagy and induce pyroptosis in corneal epithelial cells. **(A)** GSEA analysis of autophagy pathway in the control group and the KCNK5 overexpression group. **(B)** Heatmap depicting the expression of the top 10 differentially expressed genes in the control vector group, the KCNK5 vector group, the si-control group, and the siKCNK5 group ( $n = 3/\text{group}$ ). **(C)** Representative transmission electron microscopy images in the control vector group, the KCNK5 vector group, the control vector plus TNFSF10 group, and the KCNK5 vector plus TNFSF10 group. **(D)** and **(E)** Western blot and quantitative analysis results of TNFSF10, NLRP3, ASC, C-CASP1, F-GSDMD, N-GSDMD, SQSTM1, and LC3 in HCE-T cells ( $n = 3/\text{group}$ ). Scale bar = 1  $\mu\text{m}$ . Error bars = standard deviation. ns, no significant difference. \* $P < 0.05$ , \*\* $P < 0.01$ , \*\*\* $P < 0.001$ , \*\*\*\* $P < 0.0001$ .

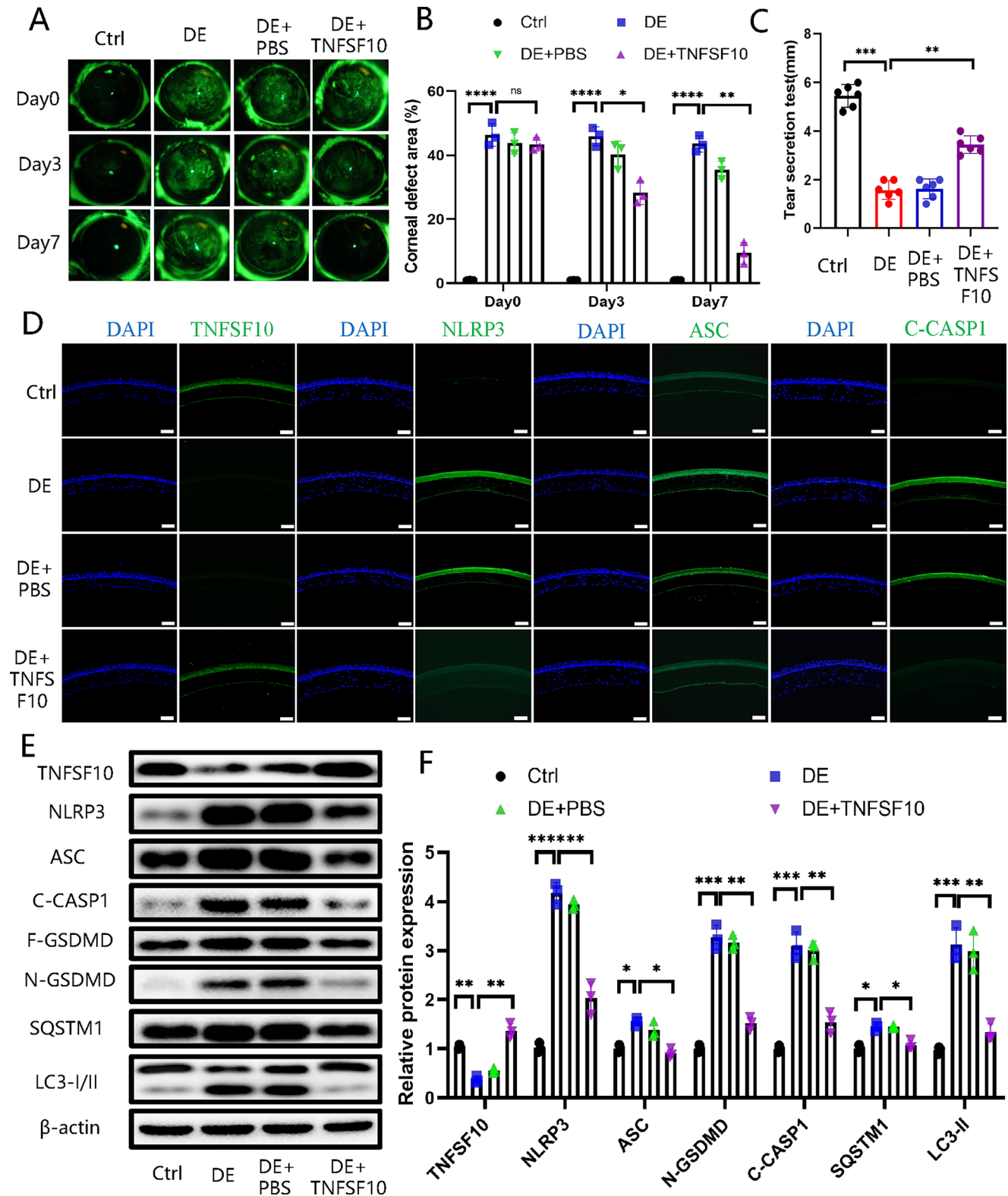


**FIGURE 7.** TNFSF10 promotes autophagy and mitigates pyroptosis in dry eye mice. **(A)** Representative corneal fluorescein staining images in dry eye mice following treatment with PBS and rhTNFSF10 subconjunctival injection treatment on days 0, 3, and 7 ( $n = 3/\text{group}$ ). **(B)** Quantitative analysis of the corneal defect area percentage ( $n = 3/\text{group}$ ). **(C)** Tear secretion test in dry eye mice ( $n = 6/\text{group}$ ). **(D)** Representative immunofluorescence staining of TNFSF10, NLRP3, ASC, and C-CASP1 in mice. **(E)** and **(F)** Western blot and quantitative analysis results of TNFSF10, NLRP3, ASC, C-CASP1, F-GSDMD, N-GSDMD, SQSTM1, and LC3 in mice ( $n = 3/\text{group}$ ). Scale bar = 100  $\mu\text{m}$ . Error bars = standard deviation. ns, no significant difference. \* $P < 0.05$ , \*\* $P < 0.01$ , \*\*\* $P < 0.001$ , \*\*\*\* $P < 0.0001$ .

## DISCUSSION

Indeed, an increasing body of evidence supports the notion that desiccation stress is a pivotal pathogenic factor in ocular surface inflammation.<sup>26–28</sup> Previous studies have underscored that pyroptosis has emerged as a fundamental mechanism in the context of dry eye inflammation.<sup>6</sup> However, how desiccation stress mediates pyroptosis in dry eye is largely unknown. In this study, we have introduced a novel mechanism, elucidating that potassium efflux, induced by the upregulation of KCNK5 in response to desiccation stress, serves as a mediator of pyroptosis in corneal epithelial cells within the context of dry eye.

Potassium efflux is a key step in inducing pyroptosis. Research reports indicate that potassium ionophores, including nigericin, induce IL-1 $\beta$  maturation in lipopolysaccharide-stimulated murine macrophages.<sup>29</sup> In our research, we also observed that nigericin could also stimulate potassium efflux-mediated pyroptosis in corneal epithelial cells. Furthermore, various stimuli, including ATP and particulate matter, can activate the NLRP3 inflammasome by reducing cytosolic potassium concentration.<sup>21</sup> Zhong et al. documented that the inhibition of S1PR3 leads to the suppression of NLRP3 and pro-IL-1 $\beta$  expression during LPS priming. This inhibition also mitigates ATP-induced NLRP3 inflammasome activation by obstructing the membrane trafficking of TWIK2 and subsequent potassium efflux.<sup>30</sup> Duan et al. have provided evidence indicating that exposure to silica results in the activation of P2  $\times$  7 ion channels, leading to intracellular potassium efflux and subsequent assembly of the NLRP3 inflammasome. This sequence of events ultimately culminates in macrophage pyroptosis and the development of pulmonary inflammation.<sup>31</sup> Indeed, it is valuable to explore the influence of additional external stimuli, such as ATP and silica, on corneal epithelial cells in forthcoming research investigations.

KCNK5 is a member of the two-pore domain potassium channel family. KCNK5 is expressed in a variety of tissues, including the central nervous system, heart, kidneys, and various other organs.<sup>32</sup> The channel's activity is regulated by various factors, including intracellular pH, membrane stretch, and various neurotransmitters.<sup>33</sup> Research on KCNK5 has indicated its potential involvement in a range of physiological and pathological processes, including the regulation of neuronal excitability, heart rhythm, and potentially its role in conditions like epilepsy and cardiac arrhythmias.<sup>34</sup> Several studies have documented the involvement of KCNK5 in the pathogenesis of various diseases. Kleinschnitz et al. reported a robust upregulation of KCNK5 in neurons following cerebral ischemia, pharmacological blockade of KCNK5 could hold therapeutic potential for preventing ischemic neurodegeneration.<sup>32</sup> Ding et al. reported an upregulation of KCNK5 in renal fibrosis tissue, knockout of KCNK5 in renal tubules could mitigate G2/M cell-cycle arrest and alleviate renal fibrosis.<sup>35</sup> In our investigation, we observed an upregulation of KCNK5 in the dry eye model, and we found that silencing KCNK5 effectively inhibited corneal epithelial pyroptosis, subsequently ameliorating dry eye symptoms. Furthermore, the overexpression of KCNK5 was also demonstrated to induce corneal epithelial pyroptosis. Quinine has had a common historical use as an antimalarial drug, and it is, in fact, a potassium channel blocker. Cooper et al. reported that quinine exhibits the potential to inhibit sperm activity, suggesting that it may be a valuable target for the development of a post-testicular male contraceptive.<sup>24</sup>

Jefferys et al. reported that quinine exhibits the capacity to prolong action potential duration and diminish firing frequency when exposed to prolonged membrane depolarization, thereby indicating its potential as a candidate for use as an anticonvulsant.<sup>36</sup> In our study, we also suggested that quinine could inhibit pyroptosis in corneal epithelial cells. Hence, it is a promising avenue to explore the development of quinine as a novel treatment for dry eye in future research.

Many studies have demonstrated that there was a close connection between autophagy and pyroptosis in multiple physiological and pathological processes.<sup>37–39</sup> Autophagy could effectively inhibit the activation of the NLRP3 inflammasome by eliminating damaged mitochondria and reducing the accumulation of reactive oxygen species, subsequently leading to the suppression of the canonical pathway of pyroptosis activation.<sup>39</sup> Our previous research established that dry eye is associated with oxidative stress-induced autophagy irregularities.<sup>16</sup> Previous studies have reported that perturbation of intracellular potassium homeostasis with the potassium-selective ionophore valinomycin promotes autophagy in several cell types.<sup>40</sup> Autophagy blocks pyroptosis through elimination of DAMPs and PAMPs and directly targeting the essential components involved in this process.<sup>41</sup> In this investigation, our findings indicate an upregulation in the activity of the potassium channel KCNK5 under desiccating stress conditions. Concurrently, cellular activity was compromised, resulting in an escalation of cell pyroptosis. Subsequent downregulation of KCNK5 led to the restoration of autophagy and a subsequent decrease in cell pyroptosis. Hence, we postulated that the heightened potassium channel activity in corneal epithelial cells under desiccation conditions led to compromised autophagy, subsequently inducing pyroptosis in corneal epithelial cells. In this study, we present the novel finding that TNFSF10 promotes autophagy, thereby mitigating corneal epithelial pyroptosis in dry eye. TNFSF10 is a member of tumor necrosis factor family, which could exert its anti-inflammatory effects by direct inhibition of T-cell activation.<sup>42</sup> Some studies have reported that TNFSF10 could induce autophagy in cancer cells.<sup>25,43</sup> Lin et al. reported that the RIPK1-mediated MAPK8/JNK activation serves as the upstream signaling pathway responsible for TNFSF10-induced cytoprotective autophagy.<sup>44</sup> In this study, we demonstrated that TNFSF10 was the downstream target of KCNK5. The precise regulatory mechanisms through which KCNK5 influences TNFSF10 expression and the underlying signaling pathways by which TNFSF10 modulates autophagy warrant further investigation. Our prior investigation has substantiated that the modulation of the IFN- $\gamma$  pathway effectively inhibits pyroptosis in corneal epithelial cells, thereby leading to the restoration of tear secretion.<sup>8</sup> Lu et al. reported that the administration of LYN-1604, an autophagy activator, resulted in the downregulation of ocular surface inflammation and a concomitant increase in tear production.<sup>45</sup> These findings suggest a nuanced and intricate interplay between ocular inflammation and the function of the lacrimal gland. Consequently, we posit that the inhibition of KCNK5 and the administration of rhTNFSF10 in dry eye mice may serve to mitigate ocular inflammation, suppress pyroptosis in lacrimal glands, and ultimately restore tear secretion. The investigation of the specific molecular mechanisms governing the influence of ocular surface inflammation on tear secretion remains an imperative avenue for future research.

In conclusion, our study reveals that KCNK5 exhibits upregulation in dry eye, and this upregulation is associ-

ated with potassium efflux and subsequent corneal epithelial cell pyroptosis. Silencing KCNK5 effectively inhibits corneal epithelial cell pyroptosis in dry eye. KCNK5 mediates TNFSF10 to impair autophagy and induce pyroptosis in dry eye. Collectively, our findings introduce a novel concept that targeting KCNK5 may represent a promising avenue for the treatment of dry eye.

### Acknowledgments

Supported by the National Natural Science Foundation of China (No. 82171015), National Natural Science Foundation of China (No. 82101083), the Science and Technology Program of Guangzhou (No. 202201020243), and the Natural Science Foundation of Guangdong Province (No. 2022A1515010445).

Disclosure: **K. Liao**, None; **H. Zeng**, None; **X. Yang**, None; **D. He**, None; **B. Wang**, None; **J. Yuan**, None

### References

- Stapleton F, Alves M, Bunya VY, et al. TFOS DEWS II epidemiology report. *Ocul Surf*. 2017;15:334–365.
- Messmer EM. The pathophysiology, diagnosis, and treatment of dry eye disease. *Dtsch Arztebl Int*. 2015;112:71–81; quiz 82.
- Pflugfelder SC, de Paiva CS. The pathophysiology of dry eye disease: what we know and future directions for research. *Ophthalmology*. 2017;124:S4–S13.
- Yu P, Zhang X, Liu N, Tang L, Peng C, Chen X. Pyroptosis: mechanisms and diseases. *Signal Transduct Target Ther*. 2021;6:128.
- Zhang J, Dai Y, Yang Y, Xu J. Calcitriol alleviates hyperosmotic stress-induced corneal epithelial cell damage via inhibiting the NLRP3-ASC-Caspase-1-GSDMD pyroptosis pathway in dry eye disease. *J Inflamm Res*. 2021;14:2955–2962.
- Chen H, Gan X, Li Y, et al. NLRP12- and NLRC4-mediated corneal epithelial pyroptosis is driven by GSDMD cleavage accompanied by IL-33 processing in dry eye. *Ocul Surf*. 2020;18:783–794.
- Cao X, Di G, Bai Y, et al. Aquaporin5 deficiency aggravates ROS/NLRP3 inflammasome-mediated pyroptosis in the lacrimal glands. *Invest Ophthalmol Vis Sci*. 2023;64:4.
- Yang X, Zuo X, Zeng H, et al. IFN- $\gamma$  facilitates corneal epithelial cell pyroptosis through the JAK2/STAT1 pathway in dry eye. *Invest Ophthalmol Vis Sci*. 2023;64:34.
- Swanson KV, Deng M, Ting JP. The NLRP3 inflammasome: molecular activation and regulation to therapeutics. *Nat Rev Immunol*. 2019;19:477–489.
- Xu Z, Chen ZM, Wu X, Zhang L, Cao Y, Zhou P. Distinct molecular mechanisms underlying potassium efflux for NLRP3 inflammasome activation. *Front Immunol*. 2020;11:609441.
- Wen X, Liao P, Luo Y, et al. Tandem pore domain acid-sensitive K channel 3 (TASK-3) regulates visual sensitivity in healthy and aging retina. *Sci Adv*. 2022;8:eabn8785.
- Caminos E, Vaquero CF, Martinez-Galan JR. Relationship between rat retinal degeneration and potassium channel KCNQ5 expression. *Exp Eye Res*. 2015;131:1–11.
- Anumanthan G, Gupta S, Fink MK, et al. KCa $_3$ .1 ion channel: a novel therapeutic target for corneal fibrosis. *PLoS One*. 2018;13:e0192145.
- Byun YS, Lee HJ, Shin S, Chung SH. Elevation of autophagy markers in Sjögren syndrome dry eye. *Sci Rep*. 2017;7:17280.
- Jeyabalan N, Pillai AM, Khamar P, Shetty R, Mohan RR, Ghosh A. Autophagy in dry eye disease: therapeutic implications of autophagy modulators on the ocular surface. *Indian J Ophthalmol*. 2023;71:1285–1291.
- Wang B, Peng L, Ouyang H, et al. Induction of DDIT4 impairs autophagy through oxidative stress in dry eye. *Invest Ophthalmol Vis Sci*. 2019;60:2836–2847.
- Yu S, Yu M, He X, Wen L, Bu Z, Feng J. KCNQ1OT1 promotes autophagy by regulating miR-200a/FOXO3/ATG7 pathway in cerebral ischemic stroke. *Aging Cell*. 2019;18:e12940.
- Chi W, Hua X, Chen X, et al. Mitochondrial DNA oxidation induces imbalanced activity of NLRP3/NLRP6 inflammasomes by activation of caspase-8 and BRCC36 in dry eye. *J Autoimmun*. 2017;80:65–76.
- Di A, Xiong S, Ye Z, et al. The TWIK2 potassium efflux channel in macrophages mediates NLRP3 inflammasome-induced inflammation. *Immunity*. 2018;49:56–65.e54.
- Panigrahi T, Shivakumar S, Shetty R, et al. Trehalose augments autophagy to mitigate stress induced inflammation in human corneal cells. *Ocul Surf*. 2019;17:699–713.
- Muñoz-Planillo R, Kuffa P, Martínez-Colón G, Smith BL, Rajendiran TM, Núñez G. K $^+$  efflux is the common trigger of NLRP3 inflammasome activation by bacterial toxins and particulate matter. *Immunity*. 2013;38:1142–1153.
- Xu J, Núñez G. The NLRP3 inflammasome: activation and regulation. *Trends Biochem Sci*. 2023;48:331–344.
- Zeng B, Huang Y, Chen S, et al. Dextran sodium sulfate potentiates NLRP3 inflammasome activation by modulating the KCa $_3$ .1 potassium channel in a mouse model of colitis. *Cell Mol Immunol*. 2022;19:925–943.
- Barfield JP, Yeung CH, Cooper TG. The effects of putative K $^+$  channel blockers on volume regulation of murine spermatozoa. *Biol Reprod*. 2005;72:1275–1281.
- Yang M, Liu L, Xie M, et al. Poly-ADP-ribosylation of HMGB1 regulates TNFSF10/TRAIL resistance through autophagy. *Autophagy*. 2015;11:214–224.
- Chen Y, Zhang X, Yang L, et al. Decreased PPAR- $\gamma$  expression in the conjunctiva and increased expression of TNF- $\alpha$  and IL-1 $\beta$  in the conjunctiva and tear fluid of dry eye mice. *Mol Med Rep*. 2014;9:2015–2023.
- Shivakumar S, Panigrahi T, Shetty R, Subramani M, Ghosh A, Jeyabalan N. Chloroquine protects human corneal epithelial cells from desiccation stress induced inflammation without altering the autophagy flux. *Biomed Res Int*. 2018;2018:7627329.
- Yu Z, Yazdanpanah G, Alam J, de Paiva CS, Pflugfelder S. Induction of innate inflammatory pathways in the corneal epithelium in the desiccating stress dry eye model. *Invest Ophthalmol Vis Sci*. 2023;64:8.
- Perregaux D, Gabel CA. Interleukin-1 beta maturation and release in response to ATP and nigericin. Evidence that potassium depletion mediated by these agents is a necessary and common feature of their activity. *J Biol Chem*. 1994;269:15195–15203.
- Wang Y, Wang C, He Q, et al. Inhibition of sphingosine-1-phosphate receptor 3 suppresses ATP-induced NLRP3 inflammasome activation in macrophages via TWIK2-mediated potassium efflux. *Front Immunol*. 2023;14:1090202.
- Zhang L, Tian J, Ma L, Duan S. Mechanistic insights into severe pulmonary inflammation caused by silica stimulation: the role of macrophage pyroptosis. *Ecotoxicol Environ Saf*. 2023;258:114975.
- Göb E, Bittner S, Bobak N, et al. The two-pore domain potassium channel KCNK5 deteriorates outcome in ischemic neurodegeneration. *Pflugers Arch*. 2015;467:973–987.
- Lesage F, Lazdunski M. Molecular and functional properties of two-pore-domain potassium channels. *Am J Physiol Renal Physiol*. 2000;279:F793–F801.

34. Li B, Rietmeijer RA, Brohawn SG. Structural basis for pH gating of the two-pore domain K(+) channel TASK2. *Nature*. 2020;586:457–462.
35. Zhang J, Chen J, Lu Y, et al. TWIK-related acid-sensitive K(+) channel 2 promotes renal fibrosis by inducing cell-cycle arrest. *iScience*. 2022;25:105620.
36. Bikson M, Id Bihi R, Vreugdenhil M, Köhling R, Fox JE, Jefferys JG. Quinine suppresses extracellular potassium transients and ictal epileptiform activity without decreasing neuronal excitability in vitro. *Neuroscience*. 2002;115:251–261.
37. Gao W, Wang X, Zhou Y, Wang X, Yu Y. Autophagy, ferroptosis, pyroptosis, and necroptosis in tumor immunotherapy. *Signal Transduct Target Ther*. 2022;7:196.
38. Lin L, Zhang MX, Zhang L, Zhang D, Li C, Li YL. Autophagy, pyroptosis, and ferroptosis: new regulatory mechanisms for atherosclerosis. *Front Cell Dev Biol*. 2021;9:809955.
39. Zhao H, Liu H, Yang Y, Wang H. The role of autophagy and pyroptosis in liver disorders. *Int J Mol Sci*. 2022;23:6208.
40. Klein B, Wörndl K, Lütz-Meindl U, Kerschbaum HH. Perturbation of intracellular K(+) homeostasis with valinomycin promotes cell death by mitochondrial swelling and autophagic processes. *Apoptosis*. 2011;16:1101–1117.
41. Guo R, Wang H, Cui N. Autophagy regulation on pyroptosis: mechanism and medical implication in sepsis. *Mediators Inflamm*. 2021;2021:9925059.
42. Chyuan IT, Tsai HF, Liao HJ, Wu CS, Hsu PN. An apoptosis-independent role of TRAIL in suppressing joint inflammation and inhibiting T-cell activation in inflammatory arthritis. *Cell Mol Immunol*. 2018;15:846–857.
43. Mills KR, Reginato M, Debnath J, Queenan B, Brugge JS. Tumor necrosis factor-related apoptosis-inducing ligand (TRAIL) is required for induction of autophagy during lumen formation in vitro. *Proc Natl Acad Sci USA*. 2004;101:3438–3443.
44. He W, Wang Q, Xu J, et al. Attenuation of TNFSF10/TRAIL-induced apoptosis by an autophagic survival pathway involving TRAF2- and RIPK1/RIP1-mediated MAPK8/JNK activation. *Autophagy*. 2012;8:1811–1821.
45. Ma S, Yu Z, Feng S, Chen H, Chen H, Lu X. Corneal autophagy and ocular surface inflammation: a new perspective in dry eye. *Exp Eye Res*. 2019;184:126–134.